One-loop electron self-energy with accelerated partial-wave expansion in the Coulomb gauge

V. A. Yerokhin ●,* Z. Harman, and C. H. Keitel ●

Max Planck Institute for Nuclear Physics, Saupfercheckweg 1, D 69117 Heidelberg, Germany

Numerical calculations of the electron self-energy without any expansion in the binding nuclear field are required in order to match the rapidly advancing precision of experimental spectroscopy. For the lightest elements, particularly hydrogen, these computations are complicated by large numerical cancelations and the slow convergence of the partial-wave expansion. Methods with accelerated convergence of the partial-wave expansion have been recently put forward [V. A. Yerokhin, K. Pachucki, and V. M. Shabaev, Phys. Rev. A **72**, 042502 (2005); J. Sapirstein and K. T. Cheng, Phys. Rev. A **108**, 042804 (2023)]. In our work we extend the accelerated-convergence methods to the previously hardly accessible region of nuclear charges $Z < 5$ and higher excited states.

I. INTRODUCTION

The electron self-energy is the leading quantum electrodynamics (QED) contribution to atomic energy levels. To match the precision of modern experiments [1–4], this effect must be calculated [5] with high accuracy and without expansion in the nuclear binding strength parameter $Z\alpha$, where Z is the nuclear charge number and α is the fine-structure constant.

Numerical calculations of the self-energy correction to all orders in $Z\alpha$ have a long history. The first such calculation was carried out by Desiderio and Johnson [6], based on the method proposed by Brown, Langer, and Schaefer [7]. A real breakthrough, however, was achieved later by Mohr [8–11], who performed accurate calculations across a broad range of ions and electron states. Despite this progress, calculations for a small range of Z values, specifically $Z < 5$, remained inaccessible for some time. It took nearly two decades to bridge this gap and extend calculations to the lightest elements, including hydrogen [12–14]. These calculations required heroic efforts, the use of multiprecision arithmetic, and the inclusion of partial-wave expansion contributions as high as several millions.

Several other methods have been reported in the literature for calculations of the electron self-energy [15–20]. The most widely used method, however, was introduced by Snyderman [21] and implemented by Blundell and Snyderman [22]. This method, sometimes referred to as the potential expansion approach, was quickly adopted by other groups [23–25] and,

most importantly, was successfully generalized for evaluations of higher-order self-energy corrections [26–29].

The potential-expansion approach produces results that are typically less accurate than those obtained by Mohr and collaborators. The main factor limiting the numerical accuracy of this approach is the uncertainty arising from the extrapolation of the partial-wave (PW) expansion of the electron propagator inside the self-energy loop. Recently it was realized that it is possible to accelerate the convergence of the PW expansion and thereby increase the accuracy achievable in this method by orders of magnitude. Specifically, there were approaches proposed by Yerokhin, Pachucki, and Shabaev (YPS) [30] and by Sapirstein and Cheng (SC) [31]. They will be referred to as the YPS and SC accelerated-convergence schemes, respectively.

Both the YPS and SC approaches are based on identities that commute the Coulomb potentials outside the free-electron propagators in the potential expansion of the Dirac-Coulomb Green function. The YPS approach was extensively used in practical calculations [32–34], but only for the first-order self-energy matrix elements and its derivatives. Extending this method to higher-order self-energy diagrams has proven to be difficult and never has been demonstrated so far. In contrast, the SC convergence-acceleration approach was already generalized to the vertex corrections [35] and to the two-loop self-energy [36].

Both the YPS and SC approaches have mostly reported results for $Z \geqslant 5$, due to large numerical cancellations that arise for lighter elements. The cause of these cancellations is well understood. Snyderman [21] demonstrated that individual self-energy contributions in Feynman gauge contain spurious terms of order $\alpha(Z\alpha)^2$, which cancel out in the sum to yield the physical result of order $\alpha(Z\alpha)^4$ and thus cause numerical cancelations for low Z. As a potential solution, Snyderman suggested using the Fried-Yennie (FY) gauge, in which these spurious terms are absent. Another possibility to avoid numerical cancelations is to use the Coulomb gauge [37–39].

---

*Contact author: vladimir.yerokhin@mpi-hd.mpg.de

In the present work we perform calculations of the electron self-energy in different gauges and demonstrate that the Coulomb gauge is the optimal choice for calculations in the low-Z region. Furthermore, we implement both the YPS and SC accelerated-convergence schemes in the Coulomb gauge and compare their performance. As a result, we establish a calculation scheme that is applicable across the entire Z region including hydrogen and arbitrary excited reference states.

The paper is organized as follows. In Sec. II we describe the generalization of the potential-expansion method for the cases of the general covariant gauge and the Coulomb gauge. This description is also the basis of the accelerated-convergence approaches. In Sec. III we discuss the YPS and SC accelerated-convergence schemes in the Coulomb gauge. In Sec. IV we describe details of our numerical implementation. Section V presents our numerical results and discussion.

The relativistic units ($\hbar = c = m = 1$) and the Heaviside charge units ($\alpha = e^2/4\pi$, $e < 0$) are used throughout this paper. We use roman style (p) for four vectors, an explicit vector notation ($\vec{p}$) for three vectors, and italic style (p) for scalars. Four vectors have the form $\mathrm{p} = (\mathrm{p}_0, \vec{p})$.

II. POTENTIAL-EXPANSION APPROACH

A. Basic formulas

The unrenormalized expression for the one-loop electron self-energy correction to an energy level of a bound state a is

$$
\Delta E_{\mathrm{SE,nren}} = 2i\alpha \int_{C_F} d\omega \int d^3x_1 d^3x_2 \, \psi_a^\dagger(\vec{x}_1) \, \alpha_\mu
$$
$$
\times \, G(\varepsilon_a - \omega, \vec{x}_1, \vec{x}_2) \, \alpha_\nu \, \psi_a(\vec{x}_2) \, D^{\mu\nu}(\omega, \vec{x}_1, \vec{x}_2),
\tag{1}
$$

where $\alpha_\mu = (1, \vec{\alpha})$, $\vec{\alpha}$ are the Dirac matrices, $G(\omega, \vec{x}_1, \vec{x}_2)$ is the Dirac-Coulomb Green's function, $D^{\mu\nu}(\omega, \vec{x}_1, \vec{x}_2)$ denotes the photon propagator (see Appendix A), and C_F is the standard Feynman integration contour. $\psi_a(\vec{x})$ is the reference-state wave function, which is a bound solution of the Dirac equation with the energy ε_a and has the form

$$
\psi_a(\vec{x}) = \begin{pmatrix} g_a(x) \, \chi_{\kappa_a \mu_a}(\hat{\vec{x}}) \\ i f_a(x) \, \chi_{-\kappa_a \mu_a}(\hat{\vec{x}}) \end{pmatrix},
\tag{2}
$$

where g_a and f_a are the radial components, $\chi_{\kappa\mu}$ are the Dirac spin-angular spinors [40], $x = |\vec{x}|$, and $\hat{\vec{x}} = \vec{x}/x$.

It is well known that the unrenormalized expression given by Eq. (1) is ultraviolet (UV) divergent and requires renormalization. Specifically, one has to regularize the UV divergencies (preferably, in a covariant manner), subtract the mass counterterm contribution, eliminate all divergent terms analytically, and obtain explicitly finite expressions that can be evaluated numerically.

The potential-expansion approach for the evaluation of the one-loop self-energy correction was introduced by Snyderman in Ref. [21]; the detailed description of this method was also presented in Ref. [25]. In this work, we concentrate on the generalization of the scheme of Ref. [25] for the cases of the general covariant gauge and the Coulomb gauge.

In the potential-expansion method, the self-energy correction after renormalization is represented as a sum of the

zero-potential, one-potential, and many-potential contributions,

$$
\Delta E_{\mathrm{SE}} = \Delta E_{\mathrm{SE}}^{(0)} + \Delta E_{\mathrm{SE}}^{(1)} + \Delta E_{\mathrm{SE}}^{(2+)},
\tag{3}
$$

where the upper index indicates the number of interactions with the binding Coulomb field inside the self-energy loop. In the following, we will consider each of these contributions in turn.

B. Zero-potential term

The zero-potential term is represented as [see Eq. (11) of Ref. [25]]

$$
\Delta E_{\mathrm{SE}}^{(0)} = \int \frac{d^3p}{(2\pi)^3} \, \overline{\psi}_a(\vec{p}) \, \Sigma_R^{(0)}(\varepsilon_a, \vec{p}) \, \psi_a(\vec{p}),
\tag{4}
$$

where $\overline{\psi} = \psi^\dagger \gamma^0$, $\psi_a(\vec{p})$ is the reference-state wave function in momentum space, and $\Sigma_R^{(0)}(\varepsilon, \vec{p})$ is the renormalized one-loop free-electron self-energy operator. The wave function in momentum space is defined as

$$
\psi_a(\vec{p}) = \int d^3x \, e^{-i\vec{p}\cdot\vec{x}} \, \psi_a(\vec{x}) = i^{-l_a} \begin{pmatrix} g_a(p) \, \chi_{\kappa_a\mu_a}(\hat{\vec{p}}) \\ f_a(p) \, \chi_{-\kappa_a\mu_a}(\hat{\vec{p}}) \end{pmatrix},
\tag{5}
$$

where $l_a = |\kappa_a + 1/2| - 1/2$.

In the general covariant gauge, the renormalized one-loop free-electron self-energy operator has the form similar to that in the Feynman gauge [cf. Eq. (A5) of Ref. [25]],

$$
\Sigma_R^{(0)}(\varepsilon, \vec{p}) = \frac{\alpha}{4\pi} [a(\rho) + \not{p} \, b(\rho)],
\tag{6}
$$

where $\not{p} = p_\mu \gamma^\mu = \varepsilon\gamma^0 - \vec{\gamma}\cdot\vec{p}$, $\rho = 1 - \varepsilon^2 + \vec{p}^2$, and the functions $a(\rho)$ and $b(\rho)$ are defined in Appendix B.

In the Coulomb gauge, the free-electron self-energy operator becomes more complex. The corresponding expression was derived by Adkins [37] and has the form

$$
\Sigma_{R,\mathrm{Coul}}^{(0)}(\varepsilon, \vec{p}) = \frac{\alpha}{4\pi} \int_0^1 dx \, du \, [a(p) + \gamma^0 \varepsilon \, b(p) + \vec{\gamma}\cdot\vec{p} \, c(p)],
\tag{7}
$$

where x and u are Feynman parameters and formulas for the functions a, b, and c are given in Appendix C.

The angular integration over $\hat{\vec{p}}$ in Eq. (4) is easily performed analytically by noting that

$$
\not{p} = \varepsilon\gamma_0 - \vec{\gamma}\cdot\vec{p} = \begin{pmatrix} \varepsilon & -\vec{\sigma}\cdot\vec{p} \\ \vec{\sigma}\cdot\vec{p} & -\varepsilon \end{pmatrix},
\tag{8}
$$

using the identity

$$
\vec{\sigma}\cdot\hat{\vec{p}} \, \chi_{\kappa\mu}(\hat{\vec{p}}) = -\chi_{-\kappa\mu}(\hat{\vec{p}}),
\tag{9}
$$

and the normalization condition

$$
\int d\hat{\vec{p}} \, \chi_{\kappa\mu}^\dagger(\hat{\vec{p}}) \, \chi_{\kappa\mu}(\hat{\vec{p}}) = 1.
\tag{10}
$$

The resulting expression for the zero-potential term in Coulomb gauge is

$$
\Delta E_{\mathrm{SE,Coul}}^{(0)} = \frac{\alpha}{32\pi^4} \int_0^\infty dp \, p^2 \int_0^1 dx \, du \, [a(p) \, (g_a^2 - f_a^2)
$$
$$
+ b(p) \, \varepsilon_a (g_a^2 + f_a^2) - c(p) \, 2p \, g_a f_a],
\tag{11}
$$

where $g_a \equiv g_a(p)$ and $f_a \equiv f_a(p)$. We note that the integration over one Feynman parameter (u) can easily be performed analytically. However, we prefer to evaluate the above expression as it stands, since it is computationally very cheap and can be performed to an arbitrary accuracy.

C. One-potential term

The one-potential term reads [see Eq. (12) of Ref. [25]]

$$\Delta E_{\text{SE}}^{(1)} = \int \frac{d^3\vec{p}'}{(2\pi)^3} \frac{d^3\vec{p}}{(2\pi)^3} \overline{\psi}_a(\vec{p}') \Gamma_R^0(\text{p}', \text{p}) V(q) \psi_a(\vec{p}),$$

(12)

where $q = |\vec{q}|$, $\vec{q} = \vec{p}' - \vec{p}$, $V(q) = -4\pi Z\alpha/q^2$ is the binding nuclear potential in momentum space, Γ_R^0 is the time component of the renormalized free-electron vertex operator Γ_R^μ, and the time components of the 4-vectors p' and p are fixed by $p_0' = p_0 = \varepsilon_a$.

In the general covariant gauge, the free-electron vertex operator has a form

$$\Gamma_R^0(\text{p}', \text{p}) = \frac{\alpha}{4\pi} \int_0^1 dy \, [\gamma^0 A + \not{p}' B + \not{p} C + \not{p}' \gamma^0 \not{p} D$$
$$+ \not{p}' \gamma^0 E + \gamma^0 \not{p} F + \not{p}' \not{p} G + H],$$

(13)

where the scalar functions A–H are obtained from formulas in Appendix D. The above expression is analogous to the Feynman-gauge representation [see Eq. (B3) of Ref. [25]], with additional functions E, F, and G that are absent in the Feynman gauge.

In the Coulomb gauge, the expression for the free-electron vertex operator becomes more complicated. The derivation of Adkins [38] yields

$$\Gamma_{R,\text{Coul}}^0(\text{p}', \text{p}) = \frac{\alpha}{4\pi} \int_0^1 dx \, du \, [\gamma^0 \mathcal{A} + \vec{\gamma} \cdot \vec{p}' \mathcal{B}$$
$$+ \vec{\gamma} \cdot \vec{p} \, \mathcal{C} + \vec{\gamma} \cdot \vec{p}' \gamma^0 \vec{\gamma} \cdot \vec{p} \, \mathcal{D}$$
$$+ \vec{\gamma} \cdot \vec{p}' \gamma^0 \mathcal{E} + \gamma^0 \vec{\gamma} \cdot \vec{p} \, \mathcal{F} + \mathcal{H}],$$

(14)

where x and u are Feynman parameters and scalar functions $\mathcal{A}$–$\mathcal{H}$ are defined in Appendix E. Note that there are only two Feynman parameters here; the third Feynman parameter s is assumed to be integrated out analytically.

In Eq. (12) we need to analytically perform integrations over all angular variables except $\xi = \hat{\vec{p}}' \cdot \hat{\vec{p}}$. The simplest way to do this is to average over the momentum projections of the reference state μ_a, using the fact that energy corrections do not depend on μ_a. After that, the action of $\not{p}$ and $\vec{\gamma} \cdot \vec{p}$ on the reference-state wave functions is worked out with the help of Eqs. (8) and (9) and the spin-angular spinors are simplified by the identity

$$\frac{4\pi}{2j+1} \sum_\mu \chi_{\kappa\mu}^\dagger(\hat{\vec{p}}') \chi_{\kappa\mu}(\hat{\vec{p}}) = P_{|\kappa+1/2|-1/2}(\xi),$$

(15)

where P_l is the Legendre polynomial.

It is convenient to introduce the integrals $X[Y]$ of basis

angular structures Y as follows:

$$\frac{1}{2j_a + 1} \sum_{\mu_a} \int d\hat{\vec{p}}' d\hat{\vec{p}} \, \overline{\psi}_a(\vec{p}') Y F(\xi) \psi_a(\vec{p})$$
$$= \frac{1}{4\pi} \int d\hat{\vec{p}}' d\hat{\vec{p}} \, X[Y] F(\xi)$$
$$= 2\pi \int_{-1}^1 d\xi \, X[Y] F(\xi),$$

(16)

where $F(\xi)$ is an arbitrary function of ξ. We obtain

$$X[\gamma^0] = g_a' g_a P_{l_a} + f_a' f_a P_{\bar{l}_a},$$
$$X[1] = g_a' g_a P_{l_a} - f_a' f_a P_{\bar{l}_a},$$
$$X[\vec{\gamma} \cdot \vec{p}] = -p \, g_a' f_a P_{l_a} - p \, f_a' g_a P_{\bar{l}_a},$$
$$X[\gamma^0 \vec{\gamma} \cdot \vec{p}] = -p \, g_a' f_a P_{l_a} + p \, f_a' g_a P_{\bar{l}_a},$$
$$X[\vec{\gamma} \cdot \vec{p}'] = -p' \, f_a' g_a P_{l_a} - p' \, g_a' f_a P_{\bar{l}_a},$$
$$X[\vec{\gamma} \cdot \vec{p}' \gamma^0] = -p' \, f_a' g_a P_{l_a} + p' \, g_a' f_a P_{\bar{l}_a},$$
$$X[\vec{\gamma} \cdot \vec{p}' \gamma^0 \vec{\gamma} \cdot \vec{p}] = p' p \, f_a' f_a P_{l_a} + p' p \, g_a' g_a P_{\bar{l}_a},$$

(17)

where $g_a' \equiv g_a(p')$, $f_a' \equiv f_a(p')$, $g_a \equiv g_a(p)$, $f_a \equiv f_a(p)$, $P_l \equiv P_l(\xi)$, $l_a = |\kappa_a + 1/2| - 1/2$, and $\bar{l}_a = |\kappa_a - 1/2| - 1/2$.

With the help of Eq. (17), the angular integration in the one-potential term is easily carried out. The resulting expression for the one-potential term in the Coulomb gauge reads

$$\Delta E_{\text{SE,Coul}}^{(1)} = -\frac{Z\alpha^2}{32\pi^5} \int_0^\infty dp' dp \int_{-1}^1 d\xi \int_0^1 dx \, du \, \frac{p'^2 p^2}{q^2}$$
$$\times \{X[\gamma^0]\mathcal{A} + X[\vec{\gamma} \cdot \vec{p}']\mathcal{B} + X[\vec{\gamma} \cdot \vec{p}]\mathcal{C}$$
$$+ X[\vec{\gamma} \cdot \vec{p}' \gamma^0 \vec{\gamma} \cdot \vec{p}]\mathcal{D} + X[\vec{\gamma} \cdot \vec{p}' \gamma^0]\mathcal{E}$$
$$+ X[\gamma^0 \vec{\gamma} \cdot \vec{p}]\mathcal{F} + X[1]\mathcal{H}\}.$$

(18)

The one-potential term in the general covariant gauge is worked out in the complete analogy with that for the Coulomb gauge.

The above expression for the one-potential term can already be calculated numerically. However, its computation is complicated by the presence of the integrable singularity of the Coulomb potential at $q \to 0$. In order to simplify numerical integrations, we subtract from the vertex operator $\Gamma_R^0(\text{p}', \text{p})$ its diagonal in p contribution, which weakens the Coulomb singularity. The subtracted contribution can then be readily evaluated by performing one momentum integration analytically. More specifically, we transform Eq. (12) as

$$\Delta E_{\text{SE}}^{(1)} = \int \frac{d^3\vec{p}' d^3\vec{p}}{(2\pi)^6} \overline{\psi}_a(\vec{p}') [\Gamma_R^0(\text{p}', \text{p}) - \Gamma_R^0(\text{p}, \text{p})] V(q) \psi_a(\vec{p})$$
$$+ \int \frac{d^3\vec{p}}{(2\pi)^3} \overline{\psi}_{Va}(\vec{p}) \Gamma_R^0(\text{p}, \text{p}) \psi_a(\vec{p}),$$

(19)

where $\psi_{Va}(\vec{p})$ is the Fourier transform of the product of the Coulomb potential and the wave function,

$$\psi_{Va}(\vec{p}) = \int d^3x \, e^{-i\vec{p} \cdot \vec{x}} V(x) \psi_a(\vec{x}).$$

(20)

A similar transformation weakening the Coulomb singularity in the one-potential term was used also in previous

investigations, notably Refs. [24,31]. We note that the Fourier transform of the product of the Coulomb potential and the wave function, $\psi_{Va}(\vec{p})$, can be readily obtained analytically, see Ref. [41] for explicit formulas.

Even after the subtraction of the diagonal in p contribution, the first term in Eq. (19) still contains some singularity at small q which complicates its numerical evaluation. In order to handle it, it is convenient to make the following change of variables [25]: $(p', p, \xi) \to (x, y, q)$, where $x = p + p'$, $y = |p - p'|$, and $q^2 = p^2 + p'^2 - 2pp'\xi$. This transforms the integral over (p', p, ξ) as follows:

$$\int_0^\infty dp' dp \int_{-1}^1 d\xi \, F(p', p, \xi) = \int_0^\infty dx \int_0^x dy \int_y^x dq \, \frac{q}{2p'p}$$
$$\times [F(p', p, \xi) + F(p, p', \xi)]. \quad (21)$$

Note the appearance of the q factor in the numerator as the consequence of the variable transformation, which softens the behavior of the integrand at small q.

D. Many-potential term

The many-potential term $\Delta E_{SE}^{(2+)}$ is obtained from Eq. (1) by applying the substitution $G(E, \vec{x}_1, \vec{x}_2) \to G^{(2+)}(E, \vec{x}_1, \vec{x}_2)$, where $G^{(2+)}(E, \vec{x}_1, \vec{x}_2)$ is the Dirac-Coulomb Green's function containing two or more interactions with the binding field. In

practical calculations $G^{(2+)}$ is often represented as

$$G^{(2+)}(E, \vec{x}_1, \vec{x}_2) = G(E, \vec{x}_1, \vec{x}_2) - G^{(0)}(E, \vec{x}_1, \vec{x}_2)$$
$$- G^{(1)}(E, \vec{x}_1, \vec{x}_2), \quad (22)$$

where $G^{(0)}(E, \vec{x}_1, \vec{x}_2)$ is the free-electron Dirac Green's function and $G^{(1)}(E, \vec{x}_1, \vec{x}_2)$ is the one-potential Dirac Green's function defined as

$$G^{(1)}(E, \vec{x}_1, \vec{x}_2) = \int d^3z \, G^{(0)}(E, \vec{x}_1, \vec{z}) V(z) G^{(0)}(E, \vec{z}, \vec{x}_2), \quad (23)$$

where $V(x) = -Z\alpha/x$ is the Coulomb potential.

We now consider the many-potential term in the general covariant gauge. The general-gauge photon propagator $D^{\mu\nu}$ can be represented (see Appendix A) as the sum of the Feynman-gauge propagator $D_F^{\mu\nu}$ and the gauge-dependent term $D_\xi^{\mu\nu}$,

$$D^{\mu\nu}(\omega, \vec{x}_1, \vec{x}_2) = D_F^{\mu\nu}(\omega, \vec{x}_1, \vec{x}_2) + \xi D_\xi^{\mu\nu}(\omega, \vec{x}_1, \vec{x}_2), \quad (24)$$

where ξ is the gauge parameter. Consequently, the many-potential term is divided into two parts,

$$\Delta E_{SE}^{(2+)} = \Delta E_F^{(2+)} + \xi \Delta E_\xi^{(2+)}. \quad (25)$$

The Feynman-gauge many-potential part is described in detail in Ref. [25], so here we concentrate on the gauge-dependent part.

Using Eq. (1), the substitution $G \to G^{(2+)}$, and formulas for the photon propagator from Appendix A, we write the gauge-dependent many-potential part as

$$\Delta E_\xi^{(2+)} = 2i\alpha \int_{C_F} d\omega \int d^3x_1 \, d^3x_2 \int \frac{d^3k}{(2\pi)^3} \frac{-1}{(\omega^2 - \vec{k}^2 + i0)^2} \psi_a^\dagger(\vec{x}_1)$$
$$\times \left[(\omega + i\vec{\alpha}_1 \cdot \vec{\nabla}_1) e^{i\vec{k}\cdot\vec{x}_1} \right] G^{(2+)}(\varepsilon_a - \omega, \vec{x}_1, \vec{x}_2) \left[(\omega - i\vec{\alpha}_2 \cdot \vec{\nabla}_2) e^{-i\vec{k}\cdot\vec{x}_2} \right] \psi_a(\vec{x}_2), \quad (26)$$

where gradients are supposed to act only on the exponential functions in the brackets. We now replace $\vec{\alpha} \cdot \vec{\nabla}$ acting on a function by the commutator of the function with the Dirac Hamiltonian h_D, $h_D(x) = -i\vec{\alpha} \cdot \vec{\nabla} + \beta m + V(x)$,

$$-i\vec{\alpha} \cdot \vec{\nabla} e^{i\vec{k}\cdot\vec{x}} = [h_D(x), e^{i\vec{k}\cdot\vec{x}}], \quad (27)$$

and evaluate the commutator, letting the Hamiltonian act on the wave function ψ_a (producing the reference-state energy ε_a) and the Green's function. We obtain

$$\Delta E_\xi^{(2+)} = 2i\alpha \int_{C_F} d\omega \int d^3x_1 \, d^3x_2 \, \psi_a^\dagger(\vec{x}_1)$$
$$\times [\omega - \varepsilon_a + h_D(x_1)] G^{(2+)}(\varepsilon_a - \omega, \vec{x}_1, \vec{x}_2) [\omega - \varepsilon_a + h_D^\dagger(x_2)] \psi_a(\vec{x}_2) \dot{D}(\omega, x_{12}), \quad (28)$$

where $\dot{D}(\omega) = -1/(2\omega)\partial/(\partial\omega)D(\omega)$, $D(\omega)$ is defined by Eq. (A1), and both Hamiltonians act on the Green's function. The action of h_D on the Green's functions is as follows:

$$[\varepsilon - h_D(x_1)] G(\varepsilon, \vec{x}_1, \vec{x}_2) = \delta^3(\vec{x}_1 - \vec{x}_2),$$
$$[\varepsilon - h_D(x_1)] G^{(0)}(\varepsilon, \vec{x}_1, \vec{x}_2) = \delta^3(\vec{x}_1 - \vec{x}_2) - V(x_1) G^{(0)}(\varepsilon, \vec{x}_1, \vec{x}_2),$$
$$[\varepsilon - h_D(x_1)] G^{(1)}(\varepsilon, \vec{x}_1, \vec{x}_2) = V(x_1) G^{(0)}(\varepsilon, \vec{x}_1, \vec{x}_2) - V(x_1) G^{(1)}(\varepsilon, \vec{x}_1, \vec{x}_2). \quad (29)$$

Therefore,

$$[\varepsilon - h_D(x_1)] G^{(2+)}(\varepsilon, \vec{x}_1, \vec{x}_2) = V(x_1) G^{(1)}(\varepsilon, \vec{x}_1, \vec{x}_2) \quad (30)$$

and, consequently,

$$[\varepsilon - h_D(x_1)] G^{(2+)}(\varepsilon, \vec{x}_1, \vec{x}_2) [\varepsilon - h_D^\dagger(x_2)] = V(x_1) [G^{(0)}(\varepsilon, \vec{x}_1, \vec{x}_2) - G^{(1)}(\varepsilon, \vec{x}_1, \vec{x}_2)] V(x_2). \quad (31)$$

We thus obtain a very simple representation for the gauge-dependent part of the many-potential term in the general covariant gauge,

$$\Delta E_{\xi}^{(2+)} = 2i\alpha \int_{C_F} d\omega \int d^3 x_1 \, d^3 x_2 \, \psi_a^{\dagger}(\vec{x}_1) V(x_1) [G^{(0)}(\varepsilon_a - \omega, \vec{x}_1, \vec{x}_2) - G^{(1)}(\varepsilon_a - \omega, \vec{x}_1, \vec{x}_2)] V(x_2) \psi_a(\vec{x}_2) \dot{D}(\omega, x_{12}). \quad (32)$$

Now we turn to the evaluation of the many-potential term in the Coulomb gauge. An expression similar to Eq. (32) can be derived also for the Coulomb gauge. However, it has the disadvantage that it cannot be easily generalized to the case of the accelerated convergence schemes, where the many-potential Green's function $G^{(2+)}$ is substituted by a more complex function. For this reason, we now perform the angular reduction of the many-potential term in the Coulomb gauge in a straightforward manner.

The simplest way to do this is to start with the unrenormalized expression (1) and employ the representation of the Green's function as a sum over the Dirac spectrum (see, e.g., Ref. [42]). Then the summation over the momentum projections is easily carried out (see Sec. 4 of Ref. [42]) and we obtain

$$\Delta E_{\text{SE,nren}} = \frac{i\alpha}{2\pi} \int_{C_F} d\omega \sum_{n,J} \frac{(-1)^{j_a + j_n + J}}{2j_a + 1} \frac{R_J(\omega, anna)}{\varepsilon_a - \omega - \varepsilon_n}, \quad (33)$$

where R_J are the standard two-body radial integrals, the same as for the one-photon exchange correction, which are very well studied in the literature. In particular, in the Coulomb gauge, expressions for the radial integrals R_J were derived in Ref. [43]. We here adopt the expressions for the Coulomb-gauge radial integrals from Ref. [44] (see Appendix B in there). Now we just rewrite those expressions in terms of the Green's function and then apply the substitution $G \rightarrow G^{(2+)}$, converting the unrenormalized expression into the many-potential term. We thus obtain the many-potential term in the Coulomb gauge as

$$\Delta E_{\text{SE,Coul}}^{(2+)} = \frac{1}{2j_a + 1} \frac{i\alpha}{2\pi} \int_{C_F} d\omega \sum_{\kappa_n, J} 2 \int_0^{\infty} dx_1 \int_0^{x_1} dx_2 \, (x_1 x_2)^2$$

$$\times \left[(2J+1)[C_J(\kappa_n, \kappa_a)]^2 g_J(0) \{G_{\kappa_n}^{(2+)}(\varepsilon_a - \omega)\}^I - \sum_{L=J-1}^{J+1} a_{JL} \, g_L(\omega) \{G_{\kappa_n}^{(2+)}(\varepsilon_a - \omega)\}_{JLL}^{II} \right.$$

$$\left. + \sqrt{J(J+1)} \, g_J^{\text{ret},1}(\omega) \{G_{\kappa_n}^{(2+)}(\varepsilon_a - \omega)\}_{J,J+1,J-1}^{II} + \sqrt{J(J+1)} \, g_J^{\text{ret},2}(\omega) \{G_{\kappa_n}^{(2+)}(\varepsilon_a - \omega)\}_{J,J-1,J+1}^{II} \right], \quad (34)$$

where the parentheses $\{\ldots\}^{I,II}$ are defined as follows:

$$\{G(\varepsilon)\}^I = g_a(x_1) G^{11}(\varepsilon, x_1, x_2) g_a(x_2) + g_a(x_1) G^{12}(\varepsilon, x_1, x_2) f_a(x_2)$$
$$+ f_a(x_1) G^{21}(\varepsilon, x_1, x_2) g_a(x_2) + f_a(x_1) G^{22}(\varepsilon, x_1, x_2) f_a(x_2), \quad (35)$$

$$\{G(\varepsilon)\}_{JLL'}^{II} = f_a(x_1) G^{11}(\varepsilon, x_1, x_2) f_a(x_2) S_{JL}(-\kappa_a, \kappa_n) S_{JL'}(-\kappa_a, \kappa_n)$$
$$- f_a(x_1) G^{12}(\varepsilon, x_1, x_2) g_a(x_2) S_{JL}(-\kappa_a, \kappa_n) S_{JL'}(\kappa_a, -\kappa_n)$$
$$- g_a(x_1) G^{21}(\varepsilon, x_1, x_2) f_a(x_2) S_{JL}(\kappa_a, -\kappa_n) S_{JL'}(-\kappa_a, \kappa_n)$$
$$+ g_a(x_1) G^{22}(\varepsilon, x_1, x_2) g_a(x_2) S_{JL}(\kappa_a, -\kappa_n) S_{JL'}(\kappa_a, -\kappa_n), \quad (36)$$

and the coefficients a_{JL} are given by

$$a_{JL} = \begin{cases} J+1, & \text{for } L = J-1, \\ 2J+1, & \text{for } L = J, \\ J, & \text{for } L = J+1. \end{cases} \quad (37)$$

In the above, C_J and S_{JL} are the standard angular coefficients given, e.g., by Eqs. (C7)–(C10) of Ref. [25], and $g_a(r)$ and $f_a(r)$ are the upper and lower radial components of the reference-state wave function. Furthermore,

$$g_l(0, x_1, x_2) = \frac{1}{2l+1} \frac{x_<^l}{x_>^{l+1}}, \quad (38)$$

$$g_l(\omega, x_1 x_2) = i\omega j_l(\omega x_<) h_l^{(1)}(\omega x_>), \quad (39)$$

$$g_l^{\text{ret},1}(\omega, x_1, x_2) = i\omega \, j_{l+1}(\omega x_<) \, h_{l-1}^{(1)}(\omega x_>), \quad (40)$$

$$g_l^{\text{ret},2}(\omega, x_1, x_2) = i\omega \, j_{l-1}(\omega x_<) \, h_{l+1}^{(1)}(\omega x_>) - \frac{2l+1}{\omega^2} \frac{x_<^{l-1}}{x_>^{l+2}}, \quad (41)$$

where $x_< = \min(x_1, x_2)$, $x_> = \max(x_1, x_2)$, and $j_l(z)$, $h_l^{(1)}(z)$ are the spherical Bessel functions. Note that the function $g_l^{\text{ret},2}$ is regular at $\omega \rightarrow 0$ despite the apparent singularity in the second term $\sim 1/\omega^2$. The disappearance of the divergent term becomes evident when one makes the small-argument expansion of the spherical Bessel functions. This cancellation, however, leads to numerical instabilities. In order to avoid
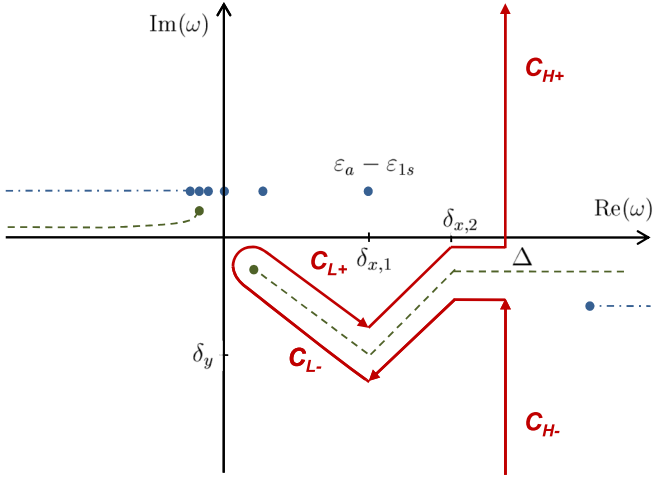
FIG. 1. Poles and the branch cuts of the integrand of the matrix element of the self-energy operator and the integration contour C_{LH} in the complex ω plane. The dashed lines (green) show the branch cuts of the photon propagator. The poles and the branch cuts of the electron propagator are shown by dots and the dashed-dot line (blue). The solid line (red) shows the integration contour C_{LH}.

them, we used the regularized functions $\bar{j}_l$ and $\bar{h}_l^{(1)}$ for small ω, as described in Ref. [44]. Note also that in Eq. (34) we used the symmetry of the integrand to restrict the integration region to $x_2 \leqslant x_1$ only.

We now turn to discussing the optimal choice of the ω integration contour, which is essential for the numerical evaluation of the many-potential term. The standard Feynman integration contour in Eq. (34) is not favorable for numerical calculations, since the Dirac Green's function is a highly oscillating function for large real ω and $x, x' \to \infty$. It is advantageous to deform the integration contour into the region of large imaginary ω since the Dirac Green's function acquires an exponentially damping factor in there.

Figure 1 shows the contour C_{LH} that we used in our calculations, which is a modification of the contour used by us earlier [25]. It consists of the low-energy part C_L and the high-energy part C_H. The low-energy part C_L is bent into the complex plane in order to avoid poles from the virtual intermediate states that are more deeply bound than the reference state. The low-energy part C_L consists of two parts, C_{L+} and C_{L-}, the first of which runs on the upper bank of the cut of the photon propagator and the second on the lower bank and in the opposite direction. Specifically, the contour C_L consist of three sections: $(0, \delta_{x,1} - i\delta_y)$, $(\delta_{x,1} - i\delta_y, \delta_{x,2})$, and $(\delta_{x,2}, \Delta)$; each of these sections are run twice in the opposite directions. The high-energy part C_H is parallel to the imaginary axis and consists of two parts, $C_{H-} = (\Delta - i\infty, \Delta - i\epsilon)$ and $C_{H+} = (\Delta + i\epsilon, \Delta + i\infty)$. The integrands for C_{H+} and C_{H-} are complex conjugated, so that it is sufficient to perform the integration over C_{H+} only and take twice the real part of the result. A more detailed discussion of the integration contour C_{LH} can be found in Sec. 5 of Ref. [42]. We note also a very useful discussion of the analytical properties of the self-energy in Ref. [8].

For the numerical evaluation of radial integrals in Eq. (34), we make the change of variables proposed by Mohr [10],

$$\int_0^\infty dx_1 \int_0^{x_1} dx_2 \, F(x_1, x_2) = \int_0^\infty dy \int_0^1 dr \, \frac{y}{a^2} F\left(\frac{y}{a}, \frac{ry}{a}\right),$$

(42)

where $r = x_2/x_1$ and $y = a x_1$, with $a = 2\sqrt{1 - \varepsilon_a^2}$. We also use some of the integration prescriptions suggested in Ref. [9], although with increased number of integration points.

III. ACCELERATED-CONVERGENCE APPROACHES

We now examine methods to enhance the convergence of the partial-wave expansion in the many-potential term. The general idea is to find an approximation for the many-potential Green's function $G^{(2+)}$, which captures the slowest-converging part of the partial-wave expansion *and* can be computed in a closed form. Then we can subtract and readd this approximation in the many-potential term, separately calculating the subtracted contribution in a closed form, without the partial-wave expansion.

There are two schemes that are able to achieve this goal, both based on an idea initially proposed by Mohr [8]. Mohr obtained an approximation for the one-potential Green's function $G^{(1)}$ by using its integral representation and commuting the Coulomb potential outside,

$$G^{(1)}(\varepsilon, \vec{x}_1, \vec{x}_2) = \int d^3z \, G^{(0)}(\varepsilon, \vec{x}_1, \vec{z}) \, V(z) \, G^{(0)}(\varepsilon, \vec{z}, \vec{x}_2)$$

$$\approx V(x_1) \int d^3z \, G^{(0)}(\varepsilon, \vec{x}_1, \vec{z}) \, G^{(0)}(\varepsilon, \vec{z}, \vec{x}_2)$$

$$= -V(x_1) \frac{\partial}{\partial \varepsilon} G^{(0)}(\varepsilon, \vec{x}_1, \vec{x}_2). \quad (43)$$

This simple approximation is based on the fact that the dominant contribution to the self-energy integral comes from the region where the radial arguments are close to each other, $\vec{x}_1 \approx \vec{x}_2$. In this region the commutators of the potential V with the free Green's function $G^{(0)}$ are small and do not contribute significantly to the partial-wave expansion.

Basing on the same idea, Sapirstein and Cheng [31] approximated the many-potential Green's function $G^{(2+)}$ as

$$G^{(2+)}(\varepsilon, \vec{x}_1, \vec{x}_2) \approx \frac{1}{2} V(x_1) \frac{\partial^2}{\partial \varepsilon^2} G^{(0)}(\varepsilon, \vec{x}_1, \vec{x}_2) \, V(x_2), \quad (44)$$

commuting the potentials outside in the two-potential term and neglecting contributions with three or more potentials.

In earlier work by one of us [30], a similar approximation was extended to all orders in the potential expansion, summing the entire series of multiple commutators. The resulting approximation of that work is equivalent to the following series:

$$G^{(2+)}(\varepsilon, \vec{x}_1, \vec{x}_2) \approx \frac{1}{2} \Omega^2 \frac{\partial^2}{\partial \varepsilon^2} G^{(0)}(\varepsilon, \vec{x}_1, \vec{x}_2)$$

$$+ \frac{1}{6} \Omega^3 \frac{\partial^3}{\partial \varepsilon^3} G^{(0)}(\varepsilon, \vec{x}_1, \vec{x}_2) + \cdots, \quad (45)$$

with $\Omega = 2Z\alpha/(x_1 + x_2)$. It is clear that the first term in Eq. (45) agrees with Eq. (44) in the limit $x_1 \to x_2$ and that the

next terms account for parts of the three- and higher-potential contributions that are not included into Eq. (44).

We now consider the two accelerated-convergence approaches in detail.

A. YPS scheme

We start with the approach introduced in Ref. [30] and referred to as the YPS scheme. It uses the following approximation $G_a^{(2+)}$ of the many-potential Green's function $G^{(2+)}$:

$$G_a^{(2+)}(\varepsilon, \vec{x}_1, \vec{x}_2) = G^{(0)}(\varepsilon + \Omega, \vec{x}_1, \vec{x}_2) - G^{(0)}(\varepsilon, \vec{x}_1, \vec{x}_2) - \Omega \frac{\partial}{\partial \varepsilon} G^{(0)}(\varepsilon, \vec{x}_1, \vec{x}_2),\tag{46}$$

with $\Omega = 2Z\alpha/(x_1 + x_2)$. Now we subtract and then readd the function $G_a^{(2+)}$ in the many-potential self-energy term, representing it as a sum of two parts,

$$\Delta E_{\text{SE}}^{(2+)} = \Delta E_{\text{acc,YPS}}^{(2+)} + \Delta E_{\text{subtr,YPS}}^{(2+)}.\tag{47}$$

The first part $\Delta E_{\text{acc,YPS}}^{(2+)}$ is obtained from $\Delta E_{\text{SE}}^{(2+)}$ given by Eq. (34) by applying the additional subtraction $G^{(2+)} \to G^{(2+)} - G_a^{(2+)}$ to the parts that have slow convergence in partial waves. Specifically, we apply this subtraction to the retarded-photon part of the high-energy contribution in Eq. (34). The low-energy contribution (corresponding to the C_L part of the integration contour) usually converges very fast and does not need any partial-wave extrapolation. The instantaneous-photon part of the high-energy contribution [induced by the first term in brackets in Eq. (34)] also converges fast and does not require acceleration.

The second term in Eq. (47), $\Delta E_{\text{subtr,YPS}}^{(2+)}$, is the subtracted contribution evaluated without partial-wave expansion. In the Feynman gauge, it was worked out in Ref. [30]. Here we evaluate this contribution in the Coulomb gauge. It reads [cf. Eq. (19) of Ref. [30]]

$$\Delta E_{\text{subtr,YPS}}^{(2+)} = -2i\alpha \int_{C_H} d\omega \int d^3x_1\, d^3x_2\, \psi_a^\dagger(\vec{x}_1)\, \alpha_i\, G_a^{(2+)}(\varepsilon_a - \omega, \vec{x}_1, \vec{x}_2)\, \alpha_j\, \psi_a(\vec{x}_2)\, D_C^{ij}(\omega, \vec{x}_1, \vec{x}_2),\tag{48}$$

where $i, j = 1, 2, 3$. Using formulas (A7) and (A8) for the photon propagator, the representation of $G_a^{(2+)}$ from Appendix F, and performing some algebra, we arrive at

$$\Delta E_{\text{subtr,YPS}}^{(2+)} = 2i\alpha \int_{C_H} d\omega \int d^3x_1\, d^3x_2\, \psi_a^\dagger(\vec{x}_1)\,[\mathcal{F}_1\, i\vec{\alpha} \cdot \vec{x}_{12} + \mathcal{F}_2\,\beta + \mathcal{F}_3]\psi_a(\vec{x}_2),\tag{49}$$

where the functions $\mathcal{F}_i = \mathcal{F}_i(x_1, x_2, x_{12})$ are given by $\mathcal{F}_1 = G_1\,(D_1 + D_2)$, $\mathcal{F}_2 = G_2\,(3D_1 - D_2)$, and $\mathcal{F}_3 = G_3\,(-3D_1 + D_2)$, and the functions $D_{1,2}$ and $G_{1,2,3}$ are defined in Appendixes A and F, respectively. The integration over all angular variables except $\xi = \hat{\vec{x}}_1 \cdot \hat{\vec{x}}_2$ is carried out analytically in the same way as for the one-potential term. We arrive at [cf. Eq. (23) of Ref. [30]]

$$\Delta E_{\text{subtr,YPS}}^{(2+)} = 4\pi i\alpha \int_{C_H} d\omega \int_0^\infty dx_1 dx_2 \int_{-1}^1 d\xi\, (x_1 x_2)^2 \left\{ \mathcal{F}_1\big[g_a(x_1)f_a(x_2)\big(x_1 P_{\bar{l}_a} - x_2 P_{l_a}\big) + f_a(x_1)g_a(x_2)\big(x_2 P_{\bar{l}_a} - x_1 P_{l_a}\big)\big] \right.$$
$$\left. + \mathcal{F}_2\big[g_a(x_1)g_a(x_2)P_{l_a} - f_a(x_1)f_a(x_2)P_{\bar{l}_a}\big] + \mathcal{F}_3\big[g_a(x_1)g_a(x_2)P_{l_a} + f_a(x_1)f_a(x_2)P_{\bar{l}_a}\big]\right\},\tag{50}$$

where $P_l = P_l(\xi)$ are the Legendre polynomials, $l_a = |\kappa_a + 1/2| - 1/2$, and $\bar{l}_a = |\kappa_a - 1/2| - 1/2$. The remaining four-dimensional integration is carried out numerically. In order to simplify the numerical integration, we make the following change of variables:

$$\int_0^\infty dx_1 dx_2 \int_{-1}^1 d\xi\, (x_1 x_2)^2\, F(x_1, x_2, \xi) = \int_0^\infty dy \int_0^1 dr \int_{x_{\min}}^{x_{\max}} dx\, \frac{ry^3 x}{a^4}\, [F(x_1, x_2, \xi) + F(x_2, x_1, \xi)],\tag{51}$$

where $r = x_2/x_1$, $y = a x_1$, $a = 2\sqrt{1 - \varepsilon_a^2}$, $x^2 = x_1^2 + x_2^2 - 2x_1 x_2 \xi$, $x_{\min} = x_1 - x_2$, and $x_{\max} = x_1 + x_2$.

B. SC scheme

The approach introduced in Ref. [31] and referred to as the SC scheme used the following approximation $G_{a,\text{SC}}^{(2+)}$ to the many-potential Green's function $G^{(2+)}$:

$$G_{a,\text{SC}}^{(2+)}(\varepsilon, \vec{x}_1, \vec{x}_2) = \frac{1}{2} V(x_1) \frac{\partial^2}{\partial \varepsilon^2} G^{(0)}(\varepsilon, \vec{x}_1, \vec{x}_2) V(x_2).\tag{52}$$

Again, one subtracts and readds $G_{a,\text{SC}}^{(2+)}$ in the many-potential contribution, separating it into two parts,

$$\Delta E_{\text{SE}}^{(2+)} = \Delta E_{\text{acc,SC}}^{(2+)} + \Delta E_{\text{subtr,SC}}^{(2+)}.\tag{53}$$

The first term $\Delta E_{\text{acc,SC}}^{(2+)}$ is obtained from Eq. (34) by applying the substitution $G^{(2+)} \to G^{(2+)} - G_{a,\text{SC}}^{(2+)}$ everywhere, whereas the subtraction term is easily represented in the momentum space as

$$\Delta E_{\text{subtr,SC}}^{(2+)} = \frac{1}{2} \int \frac{d^3p}{(2\pi)^3} \overline{\psi}_{Va}(\vec{p}) \frac{\partial^2 \Sigma_R^{(0)}(\varepsilon_a, \vec{p})}{\partial \varepsilon_a^2} \psi_{Va}(\vec{p}),\tag{54}$$

where $\psi_{Va}(\vec{p})$ is defined by Eq. (20) and the derivative of $\Sigma_R^{(0)}(\varepsilon_a, \vec{p})$ in the Coulomb gauge can be easily worked out from Eq. (C1). The numerical evaluation of the subtraction

term is fully analogous to that of the zero-potential term and does not cause any problems.

IV. NUMERICAL ASPECTS

We now provide details of our numerical computations. In the present work we assume the binding potential to be the point-nucleus Coulomb potential. The advantage of this choice is that the reference-state wave functions and the Dirac-Coulomb Green's function are known analytically. The computation of the point-nucleus bound wave functions in coordinate and momentum space is described in Ref. [45]. The radial Dirac-Coulomb Green's function is represented analytically in terms of regular and irregular Whittaker functions [45]. Our computations of the Whittaker functions follow the approach described in Ref. [25]. In the present work we upgraded the algorithms from Ref. [25] to the quadruple arithmetics (approximately 32 significant digits) to address significant numerical cancellations arising from subtracting the zero- and one-potential Green's functions in the definition of $G^{(2+)}$ for low-Z ions, especially for hydrogen.

The calculation of the zero-potential term is quite straightforward. Numerical integrations over the Feynman parameters present in the Coulomb gauge require some care because of integrable singularities that may appear around $x = 0$, $u = 0$. They are dealt with by breaking the integration region into subintervals that become increasingly smaller when approaching the singularities, e.g., $x_i = 0.001$, 0.01, and 0.1, and applying the Gauss-Legendre quadratures for each subinterval.

The computation of the one-potential term is more time consuming than that of the zero-potential term, due to the larger number of integrations. However, after the separation into the diagonal and nondiagonal in p contributions in Eq. (19) and the change of variables in the nondiagonal part given by Eq. (21), the calculation of the one-potential term becomes relatively straightforward. The numerical integrations are performed with the Gauss-Legendre quadratures. The integration of the Feynman parameter x has integrable singularities both around $x = 0$ and $x = 1$, which were dealt with in the same way as for the zero-potential contribution.

The calculation of the many-potential contribution requires the integration contour C_{LH}, with its parameters selected to optimize the numerical performance. The main parameter Δ, which separates the low- and the high-energy parts, was chosen within the interval $[3(\varepsilon_a - \varepsilon_{1s})/2, Z\alpha \varepsilon_a]$. For low Z, we usually use the upper boundary, $\Delta = Z\alpha \varepsilon_a$. For high Z and the accelerated YPS scheme, we typically decrease the parameter Δ to make the partial-wave expansion of the low-energy part converge faster. The parameter $\delta_{x,1}$ is fixed by $\delta_{x,1} = \varepsilon_a - \varepsilon_{1s}$. The choice of the parameter δ_y is a more nuanced matter. On one hand, δ_y should not be too small, as it keeps the integration contour away from the poles on the real axis, making the integrand smooth enough for high-precision numerical integration. On the other hand, δ_y should not be too large, as this could introduce numerical instabilities, given that the photon propagator on the upper side of the integration contour in the lower ω half-plane is an exponentially growing function. The compromise is empirically found to be around

$\delta_y = (\varepsilon_a - \varepsilon_{1s})/2$. The exact choice of the parameter $\delta_{x,2}$ does not matter; it was usually taken as $\delta_{x,2} = 2\delta_{x,1}$.

The many-potential term can be split into two parts—the instantaneous contribution [induced by the first term with $g_J(0)$ in brackets in Eq. (34)] and the retarded contribution [which is the remainder of Eq. (34)]. The computation of the instantaneous part is more complicated and we performed it separately. The complications are twofold. First, unlike the retarded part $g_J(\omega)$, the instantaneous part of the photon propagator $g_J(0)$ does not decay for large imaginary ω. Consequently, the accuracy of the integrand for large imaginary ω is very sensitive to the accuracy of the two-potential Green's function, which suffers from numerical cancellations in this region. Because of this, we had to use the quadruple arithmetics for its evaluation.

Second, the partial-wave expansion terms of the instantaneous part show large cancellations between different regions of ω integration. To compensate this, the numerical ω integration needs to be performed to a very high accuracy, even for high partial waves which yield very small overall contributions. Due to the presence of the instantaneous contribution, computations in the Coulomb gauge are generally more complicated than in the Feynman gauge. By contrast, the computation of the retarded contribution is very much analogous to that in the Feynman gauge described in Ref. [30].

We now turn to the evaluation of the subtraction term in the YPS scheme given by Eq. (50). After the change of variables of Eq. (51), the numerical integrations over the ω, y, and r variables are similar to that in the many-potential contribution. The integration over x is similar to the q integration in the one-potential term. However, the integrable singularity at small values of x is stronger here and requires some care. We split the integration region into several subintervals, typically, with $x = 0.01x_1$, $0.1x_1$, and apply Gauss-Legendre quadratures.

Finally, we address the extrapolation of the PW expansion, an important component of the numerical approach, as it typically determines the numerical uncertainty of the final result. We perform explicit calculations of the PW terms up to $|\kappa_{\max}| = 35$–40, then fit several last terms (typically, 4–5) to polynomials in $1/|\kappa|$ and use the results of the least-square fit to extrapolate the PW sum to infinity. We usually use several fitting functions of the form

$$\delta E_{|\kappa|} = \sum_{l=l_0}^{l_1} \frac{c_l}{|\kappa|^l}, \tag{55}$$

with free coefficients c_l and different sets of (l_0, l_1). Typically, $(l_0, l_1) = (3, 4)$, (3,5), and (3,6) were used. The convergence of each extrapolation is analyzed and the best fitting function is selected. The uncertainty is estimated on the basis of the change of the best extrapolation result when varying the $|\kappa_{\max}|$ parameter by 20%.

It should be noted that the stability of the extrapolation heavily depends on the numerical accuracy of the PW expansion terms. While higher-order PW terms are typically very small and their numerical uncertainties contribute negligibly to the error of the unextrapolated sum, they can significantly affect the extrapolated tail of the PW expansion. Generally, the more terms are included in the fitting function,

TABLE I. Individual contributions to the one-loop self-energy correction for the 1s state and $Z = 10$. Results are presented for the standard potential-expansion approach in the Feynman (Feyn), Fried-Yennie (FY), and Coulomb (Coul) gauges, and for two accelerated-convergence approaches—Acc. YPS from Ref. [30] and Acc. SC from Ref. [31]. Units are $F(Z\alpha)$.

	Standard			Acc. YPS	Acc. SC
	Feyn	FY	Coul	Coul	Coul
Zero-pot.	$-828.250\,01$	$-1.266\,74$	$5.502\,20$	$5.502\,205\,84$	$5.502\,205\,84$
One-pot.	$644.228\,50$	$6.693\,05$	$-0.278\,26$	$-0.278\,264\,37$	$-0.278\,264\,37$
Subtraction				$-0.485\,684\,60$	$-0.791\,764\,94$
$|\kappa| = 1$	$183.505\,54$	$7.549\,46$	$-0.262\,57$	$-0.023\,706\,24$	$0.222\,516\,30$
2	$3.339\,31$	$-4.713\,07$	$-0.145\,41$	$-0.062\,867\,81$	$-0.001\,734\,82$
3	$0.863\,90$	$-1.381\,76$	$-0.040\,35$	$0.001\,006\,80$	$0.001\,294\,69$
4	$0.367\,77$	$-0.668\,08$	$-0.025\,03$	$0.000\,729\,76$	$0.000\,278\,72$
5	$0.193\,45$	$-0.391\,13$	$-0.017\,49$	$0.000\,332\,88$	$0.000\,037\,32$
6	$0.114\,57$	$-0.254\,12$	$-0.012\,93$	$0.000\,163\,57$	$-0.000\,025\,88$
7	$0.073\,33$	$-0.176\,50$	$-0.009\,90$	$0.000\,088\,09$	$-0.000\,040\,49$
8	$0.049\,60$	$-0.128\,49$	$-0.007\,79$	$0.000\,051\,19$	$-0.000\,040\,59$
9	$0.034\,99$	$-0.096\,88$	$-0.006\,26$	$0.000\,031\,62$	$-0.000\,036\,50$
10	$0.025\,52$	$-0.075\,08$	$-0.005\,11$	$0.000\,020\,50$	$-0.000\,031\,61$
11	$0.019\,12$	$-0.059\,48$	$-0.004\,23$	$0.000\,013\,83$	$-0.000\,027\,01$
12	$0.014\,65$	$-0.048\,00$	$-0.003\,55$	$0.000\,009\,65$	$-0.000\,023\,00$
13	$0.011\,44$	$-0.039\,33$	$-0.003\,00$	$0.000\,006\,92$	$-0.000\,019\,61$
14	$0.009\,08$	$-0.032\,65$	$-0.002\,57$	$0.000\,005\,09$	$-0.000\,016\,78$
15	$0.007\,32$	$-0.027\,40$	$-0.002\,21$	$0.000\,003\,81$	$-0.000\,014\,43$
16…35	$0.038\,82$	$-0.177\,80$	$-0.015\,94$	$0.000\,014\,87\,(1)$	$-0.000\,099\,87\,(5)$
36…∞(extr.)	$0.007\,13\,(35)$	$-0.052\,0\,(7)$	$-0.005\,51\,(18)$	$0.000\,000\,93\,(3)$	$-0.000\,030\,47\,(15)$
Total	$4.654\,01\,(35)$	$4.653\,9\,(7)$	$4.654\,08\,(18)$	$4.654\,162\,33\,(3)$	$4.654\,162\,50\,(16)$
Ref. [19]				$4.654\,161\,9\,(1)$	

the greater the numerical accuracy of the PW terms has to be to achieve a stable extrapolation pattern.

V. NUMERICAL RESULTS

Numerical results for the one-loop self-energy correction are conveniently expressed in terms of the dimensionless function $F_{SE}(Z\alpha)$,

$$\Delta E_{SE} = mc^2 \frac{\alpha}{\pi} \frac{(Z\alpha)^4}{n^3} F_{SE}(Z\alpha). \quad (56)$$

The $Z\alpha$ expansion of the function $F_{SE}(Z\alpha)$ has the form

$$F_{SE}(Z\alpha) = L A_{41} + A_{40} + (Z\alpha) A_{50}$$
$$+ (Z\alpha)^2 [L^2 A_{62} + L A_{61} + A_{60}]$$
$$+ (Z\alpha)^3 [L A_{71} + A_{70}] + \cdots, \quad (57)$$

where $L = \ln(Z\alpha)^{-2}$. The analytical results for the coefficients A_{41}–A_{61} are summarized in Ref. [46]. The coefficient A_{60} was calculated for different states and tabulated in Refs. [47–49], whereas the coefficient $A_{71} = \pi(139/64 - \ln 2)\delta_{l,0}$ is taken from Ref. [50]. In order to assign an uncertainty to predictions based on the $Z\alpha$ expansion, we used the estimate for the unknown A_{70} coefficient of $A_{70} = 0 \pm 8 A_{60}$, where the numerical coefficient 8 was selected after comparing the $Z\alpha$-expansion and all-order results for the hydrogen $2P$ states.

We start by comparing our calculations of the one-loop self-energy correction performed within the standard potential-expansion approach in three different gauges. The

first one is the Feynman gauge, which is technically the simplest choice and is usually used in the literature. The analysis of Snyderman in Ref. [21] showed that the individual terms in Feynman gauge contain spurious contributions of order $\alpha(Z\alpha)^2$, which cause numerical cancelations for low Z. It was suggested in Ref. [21] to use the Fried-Yennie (FY) gauge, in which spurious terms are absent. Following this suggestion, we take the FY gauge as our second choice. Our third choice is the Coulomb gauge. Similarly to the FY gauge, the Coulomb gauge is known for its soft infrared properties. Explicit numerical calculations performed in Ref. [39] confirmed the absence of spurious contributions in the one-loop self-energy in this gauge.

Table I presents our numerical results obtained within these three gauges for the 1s state of H-like neon ($Z = 10$). We observe significant cancelations between the zero-, one-, and many-potential terms in the Feynman gauge. These cancelations are mostly absent in the FY gauge. However, the PW expansion in the FY gauge converges (slightly) more slowly than in the Feynman gauge. Since the convergence of the PW expansion is typically the limiting factor for the numerical accuracy of practical calculations [25], we conclude that the FY gauge does not provide computational advantages over the Feynman gauge. Nevertheless, it could still prove valuable for validating the numerical approach and the PW extrapolation procedure.

By contrast, numerical results obtained in the Coulomb gauge show both absence of spurious cancelations and some (although, small) improvement in the convergence of the PW expansion. The final results obtained in the three gauges are

TABLE II. Individual contributions to the one-loop self-energy correction for the $1s$ state of hydrogen ($Z = 1$), in the accelerated convergence scheme of Ref. [30] (Acc. YPS) and of Ref. [31] (Acc. SC), and Feynman or Coulomb gauge. Units are $F(Z\alpha)$.

| | Acc. YPS | | Acc. SC |
	Feyn	Coul	Coul
Zero-pot.	−168176.156 251	13.849 474 1	13.849 474 1
One-pot.	148579.466 946	−2.879 681 6	−2.879 681 6
Subtr.	216.681 287 (7)	−0.610 070 7 (2)	−1.127 787 5
$|\kappa| = 1$	19365.485 663	0.043 447 0	0.475 625 7
2	23.443 958	−0.091 215 7	−0.004 723 6
3	1.217 848	0.002 214 0	0.001 962 3
4	0.131 074	0.001 034 7	0.000 785 7
5	0.024 727	0.000 533 5	0.000 396 6
6	0.008 445	0.000 309 4	0.000 228 1
7	0.004 243	0.000 195 0	0.000 142 8
8	0.002 535	0.000 130 4	0.000 094 8
9	0.001 643	0.000 091 2	0.000 065 8
10	0.001 120	0.000 066 1	0.000 047 2
11	0.000 791	0.000 049 3	0.000 034 8
12	0.000 575	0.000 037 6	0.000 026 3
13	0.000 428	0.000 029 3	0.000 020 2
14	0.000 326	0.000 023 1	0.000 015 8
15	0.000 252	0.000 018 6	0.000 012 5
16...35	0.001 096 (3)	0.000 095 4 (6)	0.000 056 5 (6)
36...∞(extr.)	0.000 086 (2)	0.000 012 8 (3)	−0.000 002 1 (8)
Total	10.316 793 (8)	10.316 793 5 (7)	10.316 794 0 (10)
Ref. [13]		10.316 793 650 (1)	

consistent with each other but have different uncertainties, with the best accuracy achieved in the Coulomb gauge. We conclude that the Coulomb gauge is the optimal choice of the gauge for calculations in the low-Z region. We should note, however, that calculations in the Coulomb gauge are technically more complicated than in the Feynman gauge, so the improvement comes at a price.

Table I presents also our numerical results obtained in two approaches with the accelerated PW convergence, in the Coulomb gauge. We observe that in both cases the convergence of the PW expansion is greatly accelerated, which leads to the improvement of accuracy of the final values by three to four orders of magnitude. The convergence of the YPS scheme is somewhat better than in the SC case and its expansion terms do not change their sign. This leads to a more accurate result obtained in the YPS approach.

We now turn to the most difficult case, namely, hydrogen ($Z = 1$). So far accurate direct calculations for the electron self-energy at $Z = 1$ were reported only by Jentschura and Mohr [12–14]. Table II presents the breakdown of our numerical calculations in the YPS and SC accelerated-convergence approaches for hydrogen. For the YPS scheme, we present results both in Feynman and in Coulomb gauge. We observe large numerical cancelations in the Feynman gauge between the zero-, one-, and many-potential contributions. The advantages of the Coulomb gauge in this case are evident.

In addition to the absence of spurious contributions, the PW expansion in the Coulomb gauge exhibits a significantly (about an order of magnitude) better convergence compared to the Feynman gauge. The performance of the two schemes is very similar in this case, apparently because

terms with three and more Coulomb interactions accounted for by the YPS approach are not significant for such low Z. The YPS result is slightly more accurate than the SC one, because the SC expansion terms probably change their sign for large κ, which makes the extrapolation less stable. The results of both approaches are consistent and agree well with the more precise value obtained by Jentschura and Mohr.

An important advantage of the numerical approach of this work is that it can be applied for any Z, including the case of $Z = 1$, and not only for the ground but also for highly excited states. Table III presents our results obtained for all $n \leqslant 5$ states of hydrogen and H-like ions with $Z = 5, 10, 20$, and 40, in comparison with literature values. The listed values are obtained with the YPS approach in the Coulomb gauge, for the point nuclear model and the fine-structure fixed by $\alpha^{-1} = 137.036$, to be directly comparable with the numerical results of Mohr and collaborators.

To the best of our knowledge, our results for the $D_{5/2}$, F, and G states are the first direct calculations for $Z < 60$. (Le Bigot *et al.* [51] reported accurate results for these states but for $Z \geqslant 60$ only.) For $Z = 1$ and 5, our calculations merely cross-check the $Z\alpha$-expansion predictions, which are remarkably accurate for these excited states, but already starting with $Z = 10$ we can identify contributions due to unknown terms of order $\alpha(Z\alpha)^7$ and higher.

For nS, nP, and $nD_{3/2}$ states with $n = 3$–5 and $Z \geqslant 10$, our results in Table III are compared with those by Mohr and Kim [52]. Excellent agreement is observed in all cases, with our results typically providing 1–3 additional digits of precision. For $n \leqslant 2$ and $Z > 5$, we compare our results with the most

TABLE III. One-loop electron self-energy correction for hydrogen and hydrogenlike ions, in terms of $F(Z\alpha)$.

State	$Z = 1$	$Z = 5$	$Z = 10$	$Z = 20$	$Z = 40$
$1S_{1/2}$	10.316 793 5 (7)	6.251 627 05 (4)	4.654 162 33 (3)	3.246 255 62 (2)	2.135 228 44 (2)
	10.316 793 650 (1)[a]	6.251 627 078 (1)[a]	4.654 161 9 (1)[c]	3.246 255 7 (4)[c]	2.135 228 4 (1)[e]
$2S_{1/2}$	10.546 825 0 (4)	6.484 860 2 (4)	4.894 416 1 (2)	3.506 647 70 (5)	2.454 829 06 (3)
	10.546 825 185 (5)[a]	6.484 860 42 (1)[a]	4.894 444 4 (6)[c]	3.506 647 8 (2)[c]	2.454 829 2 (7)[e]
$3S_{1/2}$	10.605 614 0 (2)	6.543 385 8 (2)	4.952 410 3 (4)	3.563 302 3 (2)	2.508 273 0 (1)
	10.605 614 22 (5)[b]	6.543 385 98 (5)[b]	4.952 4 (2)[d]	3.563 3 (1)[d]	2.508 3 (1)[d]
$4S_{1/2}$	10.629 388 (2)	6.566 758 7 (7)	4.974 919 5 (8)	3.583 402 7 (3)	2.521 506 2 (2)
	10.629 388 4 (2)[b]	6.566 758 8 (2)[b]	4.974 9 (4)[d]	3.583 4 (1)[d]	2.521 5 (1)[d]
$5S_{1/2}$	10.641 349 (2)	6.578 390 (3)	4.985 839 (1)	3.592 309 0 (4)	2.524 604 5 (7)
			4.985 8 (6)[d]	3.592 3 (2)[d]	2.524 6 (1)[d]
$2P_{1/2}$	−0.126 395 (1)	−0.122 775 (4)	−0.114 851 (1)	−0.092 519 2 (6)	−0.031 049 9 (3)
	−0.126 396 37 (1)[a]	−0.122 774 94 (1)[a]	−0.114 852 (2)[e]	−0.092 519 0 (1)[c]	−0.031 050 0 (4)[e]
$3P_{1/2}$	−0.115 458 1 (8)	−0.111 259 (2)	−0.102 047 9 (5)	−0.076 016 1 (5)	−0.004 189 4 (7)
	−0.115 461 (4)[f]	−0.111 1 4 (4)[f]	−0.102 1 (2)[d]	−0.076 0 (1)[d]	−0.004 1 (1)[d]
$4P_{1/2}$	−0.110 424 (2)	−0.106 015 (6)	−0.096 340 (5)	−0.068 975 2 (3)	0.006 336 6 (6)
	−0.110 427 (4)[f]	−0.106 2 (5)[f]	−0.096 3 (4)[d]	−0.069 0 (2)[d]	0.006 4 (1)[d]
$5P_{1/2}$	−0.107 645 (5)	−0.103 139 (8)	−0.093 243 (4)	−0.065 255 2 (2)	0.011 561 (1)
	−0.107 648 (4)[f]	−0.103 3 (5)[f]	−0.093 3 (6)[d]	−0.065 2 (4)[d]	0.011 6 (1)[d]
$2P_{3/2}$	0.123 498 (2)	0.125 623 (2)	0.130 354 7 (9)	0.143 839 1 (4)	0.179 594 8 (1)
	0.123 498 56 (1)[a]	0.125 623 30(1)[a]	0.130 350 7(3)[c]	0.143 838 75 (4)[c]	0.179 594 9 (4)[e]
$3P_{3/2}$	0.134 414 (2)	0.136 794 (2)	0.142 085 9 (3)	0.157 185 7 (4)	0.197 728 2 (6)
	0.134 413 (2)[f]	0.136 7 (2)[f]	0.142 1 (2)[d]	0.157 2 (1)[d]	0.197 7 (1)[d]
$4P_{3/2}$	0.139 439 (2)	0.141 909 (2)	0.147 395 (2)	0.163 046 0 (2)	0.205 168 0 (4)
	0.139 439 (2)[f]	0.141 8 (2)[f]	0.147 7 (4)[d]	0.163 0 (1)[d]	0.205 2 (1)[d]
$5P_{3/2}$	0.142 215 (5)	0.144 724 (3)	0.150 297 (1)	0.166 190 8 (2)	0.208 962 2 (4)
	0.142 215 (2)[f]	0.144 6 (3)[f]	0.150 2 (6)[d]	0.166 2 (1)[d]	0.208 9 (1)[d]
$3D_{3/2}$	−0.043 019 (2)	−0.042 927 (1)	−0.042 708 (3)	−0.042 020 (2)	−0.039 617 8 (7)
	−0.043 018 3 3 (2)[f]	−0.042 929 (2)[f]	−0.042 8 (2)[d]	−0.042 0 (1)[d]	−0.039 6 (1)[d]
$4D_{3/2}$	−0.041 007 (3)	−0.040 903 (3)	−0.040 661 (4)	−0.039 880 (1)	−0.037 056 5 (5)
	−0.041 005 9 6 (2)[f]	−0.040 907 (2)[f]	−0.040 3 (4)[d]	−0.039 9 (1)[d]	−0.037 1 (1)[d]
$5D_{3/2}$	−0.039 861 (4)	−0.039 752 (3)	−0.039 496 (4)	−0.038 662 7 (7)	−0.035 604 4(5)
	−0.039 859 2 2 (2)[f]	−0.039 754 (2)[f]	−0.039 6 (6)[d]	−0.038 7 (1)[d]	−0.035 6 (1)[d]
$3D_{5/2}$	0.040 317 (1)	0.040 432 3 (6)	0.040 734 (2)	0.041 751 (2)	0.045 175 4 (5)
	0.040 316 18 (9)[f]	0.040 43 (1)[f]	0.040 73 (9)[f]	0.041 7 (7)[f]	
$4D_{5/2}$	0.042 329 (1)	0.042 460 (4)	0.042 801 (2)	0.043 959 2 (5)	0.047 931 7 (5)
	0.042 328 7 (1)[f]	0.042 46 (1)[f]	0.042 8 (1)[f]	0.043 9 (8)[f]	
$5D_{5/2}$	0.043 476 (2)	0.043 612 (6)	0.043 973 (2)	0.045 196 (2)	0.049 415 0 (2)
	0.043 475 6 (1)[f]	0.043 61 (1)[f]	0.044 0 (1)[f]	0.045 1 (8)[f]	
$4F_{5/2}$	−0.021 498 (2)	−0.021 480 (4)	−0.021 438 (4)	−0.021 309 (3)	−0.020 920 (2)
	−0.021 497 019 (7)[f]	−0.021 480 9 (9)[f]	−0.021 441 (7)[f]	−0.021 32 (6)[f]	
$5F_{5/2}$	−0.020 874 (2)	−0.020 857 (5)	−0.020 809 (10)	−0.020 668 (3)	−0.020 230 3 (7)
	−0.020 872 240 (7)[f]	−0.020 854 4 (9)[f]	−0.020 811 (7)[f]	−0.020 68 (6)[f]	
$4F_{7/2}$	0.020 170 4 (7)	0.020 193 (5)	0.020 249 (5)	0.020 450 (3)	0.021 137 (2)
	0.020 169 90 (2)[f]	0.020 192 (3)[f]	0.020 25 (2)[f]	0.020 4 (2)[f]	
$5F_{7/2}$	0.020 795 (2)	0.020 819 (6)	0.020 882 (9)	0.021 115 (3)	0.021 899 5 (4)
	0.020 794 73 (3)[f]	0.020 820 (3)[f]	0.020 89 (3)[f]	0.021 1 (2)[f]	
$5G_{7/2}$	−0.012 861 (1)	−0.012 859 (6)	−0.012 846 (6)	−0.012 805 (2)	−0.012 695 (3)
	−0.012 859 159 (3)[f]	−0.012 854 6 (3)[f]	−0.012 843 (3)[f]	−0.012 81 (2)[f]	
$5G_{9/2}$	0.012 142 (1)	0.012 148 (4)	0.012 164 (8)	0.012 224 4 (9)	0.012 441 (3)
	0.012 140927 (8)[f]	0.012 1475 (9)[f]	0.012 165 (8)[f]	0.012 23 (6)[f]	

[a]Jentschura and Mohr [13].

[b]Jentschura [14].

[c]Indelicato and Mohr [19].

[d]Mohr and Kim [52].

[e]Mohr [11].

[f]$Z\alpha$ expansion.

accurate previous calculations [11,19]. Overall, the results are in good agreement, with only minor discrepancies observed for the 1*S* and 2*S* states at $Z = 10$ with results of Indelicato and Mohr [19].

Calculations by Jentschura and Mohr [12–14] for $Z \leqslant 5$ provided extremely precise results, surpassing the accuracy achieved in the present study. However, these calculations are far more computationally expensive than those presented here and have been conducted only for a limited set of states (*nS* with $n \leqslant 4$ and $2P_j$) for ions with $Z = 1 \ldots 5$. The comparison shown in Table III provides an important confirmation of these high-precision results.

Of particular importance is hydrogen, whose theory is the basis for the determination of the Rydberg constant [53]. The current theoretical uncertainty of the 1*S*-2*S* transition frequency in hydrogen is about 1 kHz [36,53], which corresponds to a fractional accuracy of 1×10^{-7} for the 1*S* self-energy correction and 9×10^{-7} for the 2*S* state. Until now, the calculation by Jentschura and Mohr [12,13] was the only one to achieve this level of numerical accuracy for $Z = 1$. Our results provide an independent cross-check of their results.

The extended tables of our numerical results are available in the Supplemental Material [54].

VI. SUMMARY

We performed calculations of the one-loop electron self-energy in both the general covariant gauge and the Coulomb gauge. Our results demonstrated that usage of the Coulomb gauge in self-energy calculations may offer significant advantages, especially for low nuclear charges. These advantages are twofold. First, spurious contributions leading to large numerical cancelations in the low-*Z* region are absent. Second, the convergence of the partial-wave expansion becomes faster. When combined with the accelerated-convergence methods presented in Refs. [30,31], usage of the Coulomb gauge enabled us to develop a highly efficient numerical approach capable of producing accurate results for the self-energy corrections for any nuclear charge Z, including $Z = 1$, and arbitrary excited states. As a result, we extended the region of the self-energy calculations for the $D_{5/2}$, F, and G excited states as compared with previously reported calculations, improved the numerical accuracy of the literature results for some excited states and values of Z, and performed an extensive independent cross-check of previous numerical and $Z\alpha$-expansion calculations. We believe that the developed method will be useful in calculations of higher-order self-energy corrections in the low-*Z* region.

APPENDIX A: PHOTON PROPAGATOR

The photon propagator has the simplest form in the Feynman (F) gauge, where it is given by

$$D_F^{\mu\nu}(\omega, \vec{x}_1, \vec{x}_2) = -\int \frac{d^3k}{(2\pi)^3} e^{i\vec{k}\cdot(\vec{x}_1-\vec{x}_2)} \frac{g^{\mu\nu}}{\omega^2 - \vec{k}^2 + i0} = g^{\mu\nu} \frac{e^{i\sqrt{\omega^2+i0}\,x_{12}}}{4\pi x_{12}} \equiv g^{\mu\nu} D(\omega, x_{12}), \tag{A1}$$

where $x_{12} = |\vec{x}_1 - \vec{x}_2|$. In the general covariant gauge the photon propagator is written as

$$D^{\mu\nu}(\omega, \vec{x}_1, \vec{x}_2) \equiv D_F^{\mu\nu}(\omega, \vec{x}_1, \vec{x}_2) + \xi D_\xi^{\mu\nu}(\omega, \vec{x}_1, \vec{x}_2) = -\int \frac{d^3k}{(2\pi)^3} e^{i\vec{k}\cdot(\vec{x}_1-\vec{x}_2)} \left[\frac{g^{\mu\nu}}{\omega^2 - \vec{k}^2 + i0} + \xi \frac{k^\mu k^\nu}{(\omega^2 - \vec{k}^2 + i0)^2} \bigg|_{k^0=\omega} \right], \tag{A2}$$

where ξ is the gauge parameter. The particular case of the general covariant gauge is the so-called Fried-Yennie gauge, with the gauge parameter $\xi = 2$.

In atomic physics, the photon propagator typically appears in combination with Dirac matrices, as $\alpha_\mu \alpha_\nu D^{\mu\nu}$. This combination can be written in coordinate space as

$$\alpha_{1\mu}\alpha_{2\nu} D^{\mu\nu}(\omega, \vec{x}_1, \vec{x}_2) = \left[1 - \vec{\alpha}_1 \cdot \vec{\alpha}_2 + \xi(\omega + i\vec{\alpha}_1 \cdot \vec{\nabla}_1)(\omega - i\vec{\alpha}_2 \cdot \vec{\nabla}_2)\left(-\frac{1}{2\omega}\frac{\partial}{\partial\omega} \right) \right] D(\omega, x_{12}). \tag{A3}$$

The photon propagator in the Coulomb (C) gauge is given by

$$D_C^{00}(\omega, \vec{x}_1, \vec{x}_2) = \frac{1}{4\pi x_{12}}, \quad D_C^{0i}(\omega, \vec{x}_1, \vec{x}_2) = D_C^{i0}(\omega, \vec{x}_1, \vec{x}_2) = 0, \tag{A4}$$

$$D_C^{ij}(\omega, \vec{x}_1, \vec{x}_2) = \int \frac{d^3k}{(2\pi)^3} \frac{e^{i\vec{k}\cdot(\vec{x}_1-\vec{x}_2)}}{\omega^2 - \vec{k}^2 + i0} \left[\delta^{ij} - \frac{k^i k^j}{\vec{k}^2} \right], \tag{A5}$$

where $i, j = 1, 2, 3$. The combination $\alpha_\mu \alpha_\nu D_C^{\mu\nu}$ can be written as

$$\alpha_{1\mu}\alpha_{2\nu} D_C^{\mu\nu}(\omega, \vec{x}_1, \vec{x}_2) = D(0, x_{12}) - \vec{\alpha}_1 \cdot \vec{\alpha}_2 D(\omega, x_{12}) + \frac{1}{\omega^2} \vec{\alpha}_1 \cdot \vec{\nabla}_1 \vec{\alpha}_2 \cdot \vec{\nabla}_2 [D(\omega, x_{12}) - D(0, x_{12})]. \tag{A6}$$

It is sometimes convenient to transform the above expression further, to take the following form:

$$\alpha_{1\mu}\alpha_{2\nu} D_C^{\mu\nu}(\omega, \vec{x}_1, \vec{x}_2) = D(0, x_{12}) - \vec{\alpha}_1 \cdot \vec{\alpha}_2 D_1(\omega, x_{12}) + (\vec{\alpha}_1 \cdot \hat{\vec{x}}_{12})(\vec{\alpha}_2 \cdot \hat{\vec{x}}_{12}) D_2(\omega, x_{12}), \tag{A7}$$

where

$$D_1(\omega, x) = \frac{1}{4\pi\omega^2 x^3} \left[1 - (1 - i\omega x - \omega^2 x^2) e^{i\sqrt{\omega^2 + i0}\, x} \right],$$

$$D_2(\omega, x) = \frac{1}{4\pi\omega^2 x^3} \left[3 - (3 - 3i\omega x - \omega^2 x^2) e^{i\sqrt{\omega^2 + i0}\, x} \right]. \tag{A8}$$

APPENDIX B: FREE SELF-ENERGY OPERATOR IN GENERAL COVARIANT GAUGE

The free-electron self-energy operator in the general covariant gauge can be evaluated in the same way as in the Feynman gauge; see Ref. [25]. The result is

$$\Sigma_R^{(0)}(\mathrm{p}) = \frac{\alpha}{4\pi} \left[a(\rho) + \slashed{p}\, b(\rho) \right], \tag{B1}$$

where p is the four-vector $\mathrm{p} = (p_0, \vec{p})$, $\slashed{p} = p^\mu \gamma_\mu$, and the scalar functions a and b are given by

$$a(\rho) = 2(1 + \xi) + \frac{(4 + \xi)\rho}{1 - \rho} \ln \rho, \quad b(\rho) = -\frac{2 - \rho}{1 - \rho}(1 + \xi)\left(1 + \frac{\rho}{1 - \rho} \ln \rho\right), \tag{B2}$$

with $\rho = 1 - \mathrm{p}^2 = 1 - p_0^2 + \vec{p}^2$. In the Feynman gauge ($\xi = 0$), the above expressions coincide with Eqs. (A5)–(A7) of Ref. [25].

APPENDIX C: FREE SELF-ENERGY OPERATOR IN COULOMB GAUGE

The renormalized free-electron self-energy operator in the Coulomb gauge was derived by Adkins [38]. It is expressed as

$$\Sigma_{R,\,\mathrm{Coul}}^{(0)}(\mathrm{p}) = \frac{\alpha}{4\pi} \int_0^1 dx\, du\, [a + p_0 \gamma^0 b + \vec{\gamma} \cdot \vec{p}\, c], \tag{C1}$$

where

$$a = -\frac{1}{\sqrt{x}} \ln \mathcal{X} - 2 \ln \mathcal{Y}, \quad b = 2(1 - x) \ln \mathcal{Y} - \frac{1}{2}, \quad c = \frac{19}{6} - \frac{1 - x}{\sqrt{x}} \ln \mathcal{X} - 2(1 - x) \ln \mathcal{Y} + 2\sqrt{x} \ln \mathcal{Z}, \tag{C2}$$

with $\mathcal{X} = 1 + \vec{p}^2(1 - x)$, $\mathcal{Y} = 1 - (p_0^2 - \vec{p}^2)(1 - x)$, and $\mathcal{Z} = 1 - p_0^2(1 - u) + \vec{p}^2(1 - xu)$. The integration over u can easily be carried out analytically, but we prefer to keep the expression in its present form because its numerical evaluation is very cheap.

APPENDIX D: FREE-ELECTRON VERTEX OPERATOR IN GENERAL COVARIANT GAUGE

The free-electron vertex operator in the general covariant gauge can be represented as a sum of the Feynman-gauge and the gauge-dependent parts,

$$\Gamma^\mu(\mathrm{p}', \mathrm{p}) = \Gamma_F^\mu(\mathrm{p}', \mathrm{p}) + \xi\, \Gamma_\xi^\mu(\mathrm{p}', \mathrm{p}). \tag{D1}$$

The Feynman-gauge part is given in Appendix B of Ref. [25], so we concentrate here on the gauge-dependent part. The time component of the gauge-dependent part of the renormalized free-electron vertex operator is expressed as

$$\Gamma_{\xi,R}^0(\mathrm{p}', \mathrm{p}) = \frac{\alpha}{4\pi} [\gamma^0 A + \slashed{p}' B + \slashed{p} C + \slashed{p}' \gamma^0 E + \gamma^0 \slashed{p} F + \slashed{p}' \slashed{p} G + H], \tag{D2}$$

where, for $p_0' = p_0 = \varepsilon$,

$$A = (\mathrm{p}'^2 + m^2)C_{11} + (\mathrm{p}^2 + m^2)C_{12} + C_{24},$$

$$B = 2\varepsilon[(\mathrm{p}'^2 + m^2)D_{21} + (\mathrm{p}^2 + m^2)D_{23} + C_{11}],$$

$$C = 2\varepsilon[(\mathrm{p}^2 + m^2)D_{22} + (\mathrm{p}'^2 + m^2)D_{23} + C_{12}],$$

$$E = m[(-\mathrm{p}'^2 + 2\mathrm{p}' \cdot \mathrm{p})D_{21} + \mathrm{p}^2 D_{22} + 2\mathrm{p}^2 D_{23}],$$

$$F = m[\mathrm{p}'^2 D_{21} + (-\mathrm{p}^2 + 2\mathrm{p}' \cdot \mathrm{p})D_{22} + 2\mathrm{p}'^2 D_{23}],$$

$$G = -2m\varepsilon[D_{21} + D_{22} + 2D_{23}],$$

$$H = 2m\varepsilon[C_0 - \mathrm{q}^2 D_{23} + C_{11} + C_{12}]. \tag{D3}$$

Here,

$$\begin{pmatrix} D_{21} \\ D_{22} \\ D_{23} \end{pmatrix} = \int_0^1 dy \, \frac{1}{[yp' + (1-y)p]^4} \begin{pmatrix} y^2 \\ (1-y)^2 \\ y(1-y) \end{pmatrix} [-2 + (1+2Y)\ln X], \tag{D4}$$

and all other notations are from Appendix B of Ref. [25].

APPENDIX E: FREE-ELECTRON VERTEX OPERATOR IN COULOMB GAUGE

The renormalized free-electron vertex operator in the Coulomb gauge was derived by Adkins [38]. For the purposes of the present investigation, we need only the time component of the vertex operator, which is expressed as

$$\Gamma_{R,\mathrm{Coul}}^0(p', p) = \frac{\alpha}{4\pi} \int_0^1 dx\, ds\, du\, [\gamma^0 \mathcal{A} + \vec{\gamma} \cdot \vec{p}' \, \mathcal{B} + \vec{\gamma} \cdot \vec{p}\, \mathcal{C} + \vec{\gamma} \cdot \vec{p}' \gamma^0 \vec{\gamma} \cdot \vec{p}\, \mathcal{D} + \vec{\gamma} \cdot \vec{p}' \gamma^0\, \mathcal{E} + \gamma^0 \vec{\gamma} \cdot \vec{p}\, \mathcal{F} + \mathcal{H}], \tag{E1}$$

where

$$\mathcal{A} = \frac{1}{\sqrt{x}\Delta_X} \{2xu(1-u)\vec{k}^2 + (1-x)[u\vec{p}'^2 + (1-u)\vec{p}^2]\} + \frac{2}{\Delta_Y}\Bigg\{ 1 - x^2 + (xq_0 - p_0')(xq_0 - p_0) + x^2 u(1-u)k_0^2$$

$$- \frac{x}{2}(3-2x)\big[u(1-p_0'^2) + (1-u)(1-p_0^2)\big] + \vec{k}^2\bigg[-1 + \frac{x}{2} - 2x^2 u(1-u)\bigg] + \vec{p}'^2\bigg[1 - \frac{x}{2} - \frac{x}{2}(5-4x)u\bigg]$$

$$+ \vec{p}^2\bigg[1 - \frac{x}{2} - \frac{x}{2}(5-4x)(1-u)\bigg]\Bigg\} + \frac{\sqrt{x}}{\Delta_Z}(-2\vec{p}' \cdot \vec{p}) + \frac{2x\sqrt{x}s}{\Delta_Z^2}(-\vec{p}' \cdot \vec{p})\vec{q}^{\,2} - \ln\Delta, \tag{E2}$$

$$\mathcal{B} = \frac{1}{\sqrt{x}\Delta_X} k_0 u(-1 - x + 2xu) + \frac{2}{\Delta_Y}(-u)x(2xq_0 - p_0' - p_0) + \frac{\sqrt{x}}{\Delta_Z}(sq_0 - p_0)$$

$$+ \frac{2x\sqrt{x}s}{\Delta_Z^2} u[\vec{p}' \cdot \vec{q}\,(sq_0 - p_0) + \vec{p} \cdot \vec{q}\,(sq_0 - p_0')], \tag{E3}$$

$$\mathcal{C} = \frac{1}{\sqrt{x}\Delta_X} k_0(1-u)(1 - x + 2xu) + \frac{2}{\Delta_Y}(u-1)x(2xq_0 - p_0' - p_0) + \frac{\sqrt{x}}{\Delta_Z}(sq_0 - p_0')$$

$$+ \frac{2x\sqrt{x}s}{\Delta_Z^2}(1-u)[\vec{p}' \cdot \vec{q}\,(sq_0 - p_0) + \vec{p} \cdot \vec{q}\,(sq_0 - p_0')], \tag{E4}$$

$$\mathcal{D} = -\frac{1-x}{\sqrt{x}\Delta_X} - \frac{2}{\Delta_Y} + \frac{2\sqrt{x}}{\Delta_Z} + \frac{2x\sqrt{x}s}{\Delta_Z^2}\vec{q}^{\,2}, \tag{E5}$$

$$\mathcal{E} = -\frac{1}{\sqrt{x}\Delta_X} + \frac{\sqrt{x}}{\Delta_Z} + \frac{2x\sqrt{x}s}{\Delta_Z^2}(-u)\vec{q} \cdot \vec{k}, \tag{E6}$$

$$\mathcal{F} = -\frac{1}{\sqrt{x}\Delta_X} + \frac{\sqrt{x}}{\Delta_Z} + \frac{2x\sqrt{x}s}{\Delta_Z^2}(1-u)\vec{q} \cdot \vec{k}, \tag{E7}$$

$$\mathcal{H} = \frac{1}{\sqrt{x}\Delta_X} k_0(1-2u) + \frac{2}{\Delta_Y}(2xq_0 - p_0' - p_0), \tag{E8}$$

where $q = up' + (1-u)p$ and $k = p - p'$. Furthermore, $\Delta = 1 - u(1-u)(k_0^2 - \vec{k}^2)$,

$$\Delta_X = 1 - u(1-u)(k_0^2 - x\vec{k}^2) + (1-x)[u\vec{p}'^2 + (1-u)\vec{p}^2], \tag{E9}$$

$$\Delta_Y = x - xu(1-u)(k_0^2 - \vec{k}^2) + (1-x)u(1 - p_0'^2 + \vec{p}'^2) + (1-x)(1-u)(1 - p_0^2 + \vec{p}^2), \tag{E10}$$

$$\Delta_Z = s - su(1-u)(k_0^2 - x\vec{k}^2) + (1-s)u(1 - p_0'^2) + (1-s)(1-u)(1 - p_0^2) + (1-xs)[u\vec{p}'^2 + (1-u)\vec{p}^2]. \tag{E11}$$

Integration over one of the Feynman parameters (s) in the above formulas can be easily carried out analytically in terms of basic integrals J_{01}, J_{11}, J_{12}, and J_{22}, where

$$J_{ik} = \int_0^1 ds \, \frac{s^i}{(1 + sZ)^k}, \tag{E12}$$

and Z comes from representing $\Delta_Z = \Delta_{Z,s=0}\,(1 + sZ)$.

APPENDIX F: APPROXIMATE MANY-POTENTIAL GREEN'S FUNCTION $G_a^{(2+)}$

Using the closed-form formula for the free Green's function [8]

$$G^{(0)}(E, \vec{x}_1, \vec{x}_2) = -\left[\left(\frac{c}{x_{12}} + \frac{1}{x_{12}^2}\right) i\,\vec{\alpha} \cdot \vec{x}_{12} + \beta + E\right] \frac{e^{-c\,x_{12}}}{4\pi x_{12}}, \tag{F1}$$

where $\vec{\alpha}$ and β are the Dirac matrices and $c = \sqrt{1 - E^2}$, we express $G_a^{(2+)}$ in Eq. (46) as

$$G_a^{(2+)}(E, \vec{x}_1, \vec{x}_2) = i\vec{\alpha} \cdot \vec{x}_{12}\, G_1(E, \Omega, x_{12}) + \beta\, G_2(E, \Omega, x_{12}) + G_3(E, \Omega, x_{12}), \tag{F2}$$

with

$$G_1(E, \Omega, x) = -\frac{1}{4\pi x}\left[e^{-c'x}\left(\frac{c'}{x} + \frac{1}{x^2}\right) - e^{-cx}\left(\frac{c}{x} + \frac{1}{x^2} + \Omega E\right)\right],$$

$$G_2(E, \Omega, x) = -\frac{1}{4\pi x}\left[e^{-c'x} - e^{-cx}\left(1 + \Omega\frac{E}{c}x\right)\right],$$

$$G_3(E, \Omega, x) = -\frac{1}{4\pi x}\left[e^{-c'x}(E + \Omega) - e^{-cx}\left(E + \Omega + \Omega\frac{E^2}{c}x\right)\right], \tag{F3}$$

and $c' = \sqrt{1 - (E + \Omega)^2}$.

---

[1] R. Loetzsch, H. Beyer, L. Duval, U. Spillmann, D. Banaś, P. Dergham, F. Kröger, J. Glorius, R. Grisenti, M. Guerra *et al.*, Nature (London) **625**, 673 (2024).

[2] P. Pfäfflein, G. Weber, S. Allgeier, Z. Andelkovic, S. Bernitt, A. I. Bondarev, A. Borovik, L. Duval, A. Fleischmann, O. Forstner *et al.*, arXiv:2407.04166.

[3] T. Gaßner, M. Trassinelli, R. Heß, U. Spillmann, D. Banaś, K.-H. Blumenhagen, F. Bosch, C. Brandau, W. Chen, C. Dimopoulou *et al.*, New J. Phys. **20**, 073033 (2018).

[4] S. Kraft-Bermuth, V. Andrianov, A. Bleile, A. Echler, P. Egelhof, P. Grabitz, S. Ilieva, O. Kiselev, C. Kilbourne, D. McCammon *et al.*, J. Phys. B **50**, 055603 (2017).

[5] P. Indelicato, J. Phys. B **52**, 232001 (2019).

[6] A. M. Desiderio and W. R. Johnson, Phys. Rev. A **3**, 1267 (1971).

[7] G. E. Brown, J. S. Langer, and G. W. Schaefer, Proc. R. Soc. London A **251**, 92 (1959).

[8] P. J. Mohr, Ann. Phys. (NY) **88**, 26 (1974).

[9] P. J. Mohr, Ann. Phys. (NY) **88**, 52 (1974).

[10] P. J. Mohr, Phys. Rev. A **26**, 2338 (1982).

[11] P. J. Mohr, Phys. Rev. A **46**, 4421 (1992).

[12] U. D. Jentschura, P. J. Mohr, and G. Soff, Phys. Rev. Lett. **82**, 53 (1999).

[13] U. D. Jentschura, P. J. Mohr, and G. Soff, Phys. Rev. A **63**, 042512 (2001).

[14] U. D. Jentschura and P. J. Mohr, Phys. Rev. A **69**, 064103 (2004).

[15] P. Indelicato and P. J. Mohr, Phys. Rev. A **46**, 172 (1992).

[16] H. Persson, I. Lindgren, and S. Salomonson, Phys. Scr. **T46**, 125 (1993).

[17] H. M. Quiney and I. P. Grant, Phys. Scr. **T46**, 132 (1993).

[18] L. N. Labzowsky and I. A. Goidenko, J. Phys. B **30**, 177 (1997).

[19] P. Indelicato and P. J. Mohr, Phys. Rev. A **58**, 165 (1998).

[20] J. Zamastil and V. Patkóš, Phys. Rev. A **86**, 042514 (2012).

[21] N. J. Snyderman, Ann. Phys. (NY) **211**, 43 (1991).

[22] S. A. Blundell and N. J. Snyderman, Phys. Rev. A **44**, R1427(R) (1991).

[23] K. T. Cheng, W. R. Johnson, and J. Sapirstein, Phys. Rev. A **47**, 1817 (1993).

[24] A. Mitrushenkov, L. Labzowsky, I. Lindgren, H. Persson, and S. Salomonson, Phys. Lett. A **200**, 51 (1995).

[25] V. A. Yerokhin and V. M. Shabaev, Phys. Rev. A **60**, 800 (1999).

[26] H. Persson, S. Salomonson, P. Sunnergren, and I. Lindgren, Phys. Rev. Lett. **76**, 204 (1996).

[27] S. A. Blundell, K. T. Cheng, and J. Sapirstein, Phys. Rev. A **55**, 1857 (1997).

[28] V. A. Yerokhin, A. N. Artemyev, T. Beier, G. Plunien, V. M. Shabaev, and G. Soff, Phys. Rev. A **60**, 3522 (1999).

[29] V. A. Yerokhin, Phys. Rev. A **62**, 012508 (2000).

[30] V. A. Yerokhin, K. Pachucki, and V. M. Shabaev, Phys. Rev. A **72**, 042502 (2005).

[31] J. Sapirstein and K. T. Cheng, Phys. Rev. A **108**, 042804 (2023).

[32] V. A. Yerokhin, Phys. Rev. A **83**, 012507 (2011).

[33] V. A. Yerokhin, K. Pachucki, Z. Harman, and C. H. Keitel, Phys. Rev. Lett. **107**, 043004 (2011).

[34] V. A. Yerokhin, K. Pachucki, M. Puchalski, C. H. Keitel, and Z. Harman, Phys. Rev. A **102**, 022815 (2020).

[35] A. V. Malyshev, E. A. Prokhorchuk, and V. M. Shabaev, Phys. Rev. A **109**, 062802 (2024).

[36] V. A. Yerokhin, Z. Harman, and C. H. Keitel, Phys. Rev. Lett. **133**, 251803 (2024).

[37] G. S. Adkins, Phys. Rev. D **27**, 1814 (1983).

[38] G. S. Adkins, Phys. Rev. D **34**, 2489 (1986).

[39] D. Hedendahl and J. Holmberg, Phys. Rev. A **85**, 012514 (2012).

[40] M. E. Rose, *Relativistic Electron Theory* (John Wiley & Sons, New York, 1961).

[41] P. J. Mohr, G. Plunien, and G. Soff, Phys. Rep. **293**, 227 (1998).

[42] V. A. Yerokhin and A. V. Maiorova, Symmetry **12**, 800 (2020).

[43] J. B. Mann and W. R. Johnson, Phys. Rev. A **4**, 41 (1971).

[44] V. A. Yerokhin, C. H. Keitel, and Z. Harman, Phys. Rev. A **104**, 022814 (2021).

[45] P. J. Mohr and B. N. Taylor, Rev. Mod. Phys. **72**, 351 (2000).

[46] V. A. Yerokhin, K. Pachucki, and V. Patkóš, Ann. Phys. (Leipzig) **531**, 1800324 (2019).

[47] K. Pachucki, Ann. Phys. (NY) **226**, 1 (1993).

[48] U. Jentschura and K. Pachucki, Phys. Rev. A **54**, 1853 (1996).

[49] E.-O. Le Bigot, U. D. Jentschura, P. J. Mohr, P. Indelicato, and G. Soff, Phys. Rev. A **68**, 042101 (2003).

[50] S. G. Karshenboim, Z. Phys. D **39**, 109 (1997).

[51] E.-O. Le Bigot, P. Indelicato, and P. J. Mohr, Phys. Rev. A **64**, 052508 (2001).

[52] P. J. Mohr and Y.-K. Kim, Phys. Rev. A **45**, 2727 (1992).

[53] E. Tiesinga, P. J. Mohr, D. B. Newell, and B. N. Taylor, Rev. Mod. Phys. **93**, 025010 (2021).

[54] See Supplemental Material at http://link.aps.org/supplemental/10.1103/PhysRevA.111.012802 for the extended tables of our numerical results.